Curvature singularity and film-skating during drop impact

Laurent Duchemin[1] and Christophe Josserand[2]
[1]*IRPHE, CNRS & Aix-Marseille Université, 49 rue Joliot-Curie, 13013 Marseille, France*
[2]*Institut D'Alembert, CNRS & UPMC (Univ. Paris 06), UMR 7190, Case 162, 4 place Jussieu, F-75005 Paris, France*

(Received 4 June 2011; accepted 26 August 2011; published online 19 September 2011)

We study the influence of the surrounding gas in the dynamics of drop impact on a smooth surface. We use an axisymmetric model for which both the gas and the liquid are incompressible; lubrication regime applies for the gas film dynamics and the liquid viscosity is neglected. In the absence of surface tension a finite time singularity whose properties are analysed is formed and the liquid touches the solid on a circle. When surface tension is taken into account, a thin jet emerges from the zone of impact, skating above a thin gas layer. The thickness of the air film underneath this jet is always smaller than the mean free path in the gas suggesting that the liquid film eventually wets the surface. We finally suggest an aerodynamical instability mechanism for the splash. © *2011 American Institute of Physics*. [doi:10.1063/1.3640028]

Drop impact is present in many surface flows and diphasic dynamics. It is crucial to our understanding of atomization, ink-jet printing or deposition for instance,[1] as well as for environmental issues such as raindrop impact erosion or aerosol spreading.[2] The general situation involves an almost spherical drop impacting on a dry or wet solid surface. A splash is observed for strong impact conditions, whereas a gentle spreading of the drop is seen otherwise. On a dry substrate as considered further on, the splash is characterized by a corolla that detaches from the solid substrate forming a corona shape from which droplets can eventually detach.[3] This complex dynamics involves various parameters which can highly influence the transition between these two regimes: primarily viscous and capillary effects are invoked, quantified by the Reynolds and the Weber numbers respectively. The impacted surface is also important: in particular, the roughness of the surface can control the splash formation[4,5] as enhanced with textured surfaces.[6] Recently, the surrounding gas, often neglected in these problems, has been shown to be crucial since the splashing observed at atmospheric pressure disappears when the ambient gas pressure is lowered.[7] Despite the few models already proposed to explain this striking effect, invoking in particular compressibility of the surrounding gas[7] or the entrapment of a (compressible) gas bubble by air cushioning,[8,9] a complete understanding for the mechanism of the splash formation is still lacking. The aim of this paper is thus to disentangle the role of the surrounding gas for the drop impact on solid surfaces in the limits, where the viscosity of the liquid of the drop can be neglected and where both fluid can be considered incompressible.

We consider the impact of an incompressible liquid drop of radius R, density ρ_l, with vertical velocity V on a solid substrate (see Figure 1). The gas is taken incompressible of density ρ_g, dynamic viscosity η and surface tension γ. Although in the experiments[7] the gas is clearly in a compressible regime beneath the drop due to the large pressures created by the air cushioning, we argue that the gas compressibility might not be crucial to understand the splashing transition since it does not change the general structure of the equations. Gravity can be neglected since the Froude numbers ($Fr = V^2/gR$) are always above 10^2 and axisymmetric approximation can be safely assumed at short time. We note $t = 0$, the time at which the drop would touch the wall in the absence of the surrounding gas. The dominant effect of the gas lies in the dynamics of the viscous thin gas film underneath the drop. In this situation, the viscous boundary layer in the liquid created by the gas shear flow is small and the liquid velocity can be approximated by a potential flow while the dynamics of the gas layer follows the lubrication equation.[8,11] Our model is thus similar to the 2D approach addressed recently,[8,11,12] where a liquid parabola impacts a solid surface, but with crucial differences: (1) it is axisymmetric; (2) a spherical drop impacts; (3) we use a curvilinear description of the interface which allows for the description of the jet.

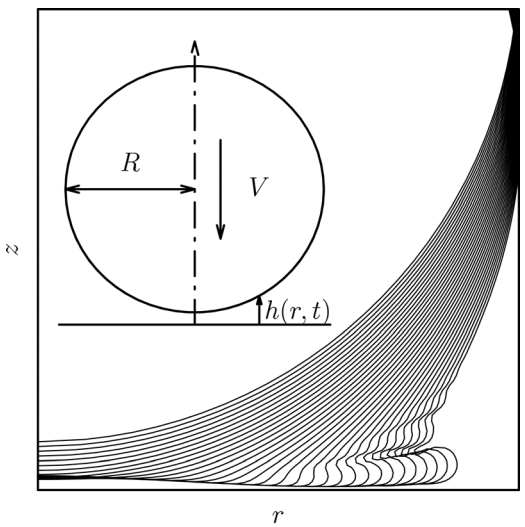

FIG. 1. Sketch of the impacting drop.

Finally, the liquid drop and the gas film dynamics are given by the following dimensionless set of equations in the cylindrical coordinates (r, z)

$$(\partial\Omega)\partial_t\varphi + \frac{1}{2}\nabla\varphi^2 + p + \frac{1}{\mathrm{We}}\kappa = C(t), \tag{1}$$

$$(\partial\Omega)\partial_t h = \frac{1}{12r\mathrm{St}}\partial_r(rh^3\partial_r p), \tag{2}$$

$$(\partial\Omega)\partial_t h = \partial_z\varphi - \partial_r\varphi\partial_r h, \tag{3}$$

$$(\Omega)\Delta\varphi = 0, \tag{4}$$

where φ is the velocity potential in the drop $(\mathbf{u}(r,z,t) = \nabla\varphi(r,z,t))$, Ω is the liquid domain, $\partial\Omega$ is the boundary of the drop and p is the lubrication pressure in the gas. The lengths have been rescaled by R, velocities by V, densities by ρ_l and the gas pressure by $\rho_l V^2$. The full interface $\{r(s,t), z(s,t)\}$ is indexed by the curvilinear coordinate s and κ is the mean curvature of the interface. This set of equations introduces the two dimensionless numbers of the problem, the Weber and Stokes numbers

$$\mathrm{We} = \frac{\rho_l R V^2}{\gamma} \quad \text{and} \quad \mathrm{St} = \frac{\eta}{\rho_l V R}.$$

Remarkably, general experimental conditions correspond to $\mathrm{St} \ll 1$ as considered further on. The incompressibility condition (4) joint with the Bernoulli equation at the drop interface (1) describes the liquid potential flow. This dynamics is coupled with the surrounding gas flow through the interface advection Equation (3) and the pressure, given in the thin film by the lubrication approximation (2). Notice that lubrication is only valid where the slope of the interface is small enough, otherwise a free surface condition ($p = P_0$) has to be applied in Bernoulli equation: lubrication equation is written in terms of the arc-length along the interface, then it is solved from the axis of symmetry to the first point where the interface is vertical (at short-time, this point is the equator of the drop; once the jet is formed, it is the radial extension of the jet). In this region where $\partial_r h \gg 1$, the radial pressure gradient decays like $1/h^2$. After this point, free surface condition is applied.

The numerical method proceeds as follows: Laplace's Equation (4) is solved using a boundary integral method, the pressure is calculated through the lubrication Equation (2),[13] the interface and the velocity potential are advanced in time using the kinematic condition (3) and Bernoulli Equation (1) respectively.

A sequence of snapshots of the drop impact is shown in Figure 1 for $\mathrm{We} = 23.7$ and $\mathrm{St} = 1.35 \times 10^{-3}$. The drop deforms as it approaches the wall and a dimple appears underneath. Then a quasi-horizontal liquid jet expands rapidly. We observe in Figure 1 that the liquid never touches the wall and the jet "skates" on a thin gas layer! This is consistent with the general property of viscous film that cannot break-up in a finite-time.[14] However, this is not the case in the absence of surface tension where corner like interface can be created as described below.

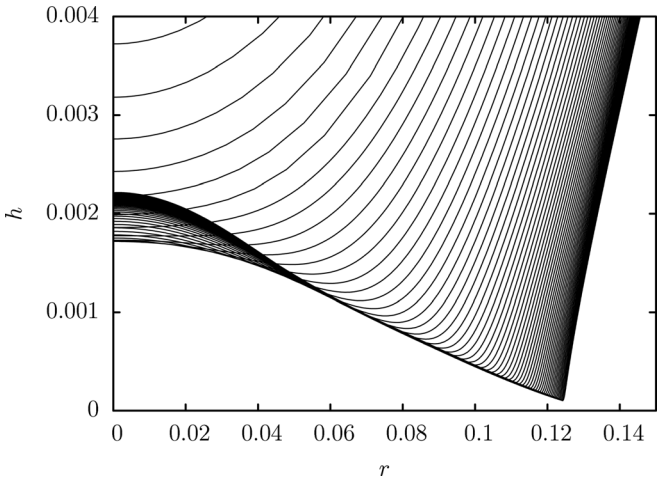

FIG. 2. Interface profile near the singularity for a drop impact with zero surface tension and $\mathrm{St} = 1.35 \times 10^{-3}$.

Finite time singularity for $\mathrm{We} = \infty$: as observed in 2D,[8,11,12] the dynamics exhibits a finite time singularity in the zero surface tension case, as shown in Figure 2. It corresponds as $t \to t_0$ to a corner like interface located at $r_c(t) \to r_0$ where the curvature $\kappa_0(t)$ diverges as the film thickness $h_0(t)$ vanishes. Similarly, the maximum pressure $p_0(t)$ is located in $r_p(t) \neq r_c(t)$ and diverges when $t \to t_0$ (and $r_p(t) \to r_0$), following:

$$p_0 \propto h_0^{-\frac{1}{2}\pm 0.05} \quad \kappa_0 \propto h_0^{-2\pm 0.05},$$

as presented in Figure 3. The radial position $r_0(t)$ of $h_0(t)$ follows approximately the geometrical intersection between the undeformed drop and the solid wall ($r_0 \sim \sqrt{2t}$ and $\dot{r}_0 = 1/\sqrt{2t}$). Using the typical gas film thickness $H^* = \mathrm{St}^{2/3}$ by balancing the drop inertia and the lubrication pressure,[8] one can estimate $t_0 \sim H^*$ and thus $r_0 \sim \mathrm{St}^{1/3}$ ($\dot{r}_0 \sim \mathrm{St}^{-1/3}$) at the singularity, in good agreement with the numerical results.

To understand the properties of this singularity, we seek self-similar solutions of the form: $\tilde{h}(r,t) = h_0(t)H(R)$,

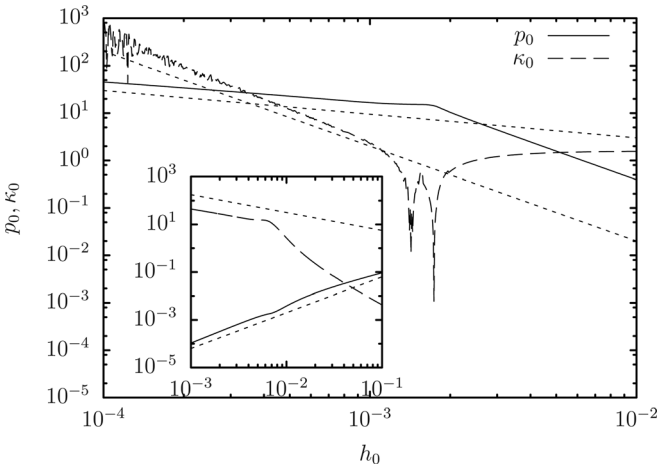

FIG. 3. p_0 and κ_0 as functions of h_0. The two dotted lines show respectively the $h_0^{-\frac{1}{2}}$ and h_0^{-2} scalings. The inset shows $h_0(t)$ and $p_0(t)$ as function of $(t_0 - t)$ close to the singularity, with the fitted scalings $h_0(t) \propto (t_0 - t)^{3/2}$ and $p_0(t) \propto (t_0 - t)^{-3/4}$.

$\tilde{p}(r,t) = p_0(t)P(R)$, and $\tilde{\varphi}(r,t) = \varphi_0(t)\Phi(R,Z)$, where $R = (r - r_0(t))/l(t)$ and $Z = z/l(t)$. Near the singularity, the spatial variations are seen numerically slower than $(t_0 - t)$ (see caption of Figure 3), so that the time derivatives shall be replaced by $(h_0\dot{r}_0/l(t))\partial_R$ and Eqs. (1)–(4) give at dominant order, after dropping the tilde

$$(\partial\Omega) - \frac{\varphi_0\dot{r}_0}{l}\partial_R\Phi + \frac{1}{2}\frac{\varphi_0^2}{l^2}\nabla\Phi^2 + p_0P = C(t), \tag{5}$$

$$(\partial\Omega) - \frac{h_0\dot{r}_0}{l}H' = \frac{h_0^3 p_0 (H^3P')'}{12\,\mathrm{St}\,l^2}, \tag{6}$$

$$(\partial\Omega) - \frac{h_0\dot{r}_0}{l}H' = \frac{\varphi_0}{l}(\partial_Z\Phi - \frac{h_0}{l}H'\partial_R\Phi), \tag{7}$$

$$(\Omega)\Delta\Phi = 0. \tag{8}$$

Taking $\dot{r}_0 = \mathrm{St}^{-1/3}$, we identify two regimes based on the relevant terms in Eq. (7).

Regime I: $h_0 \ll l$: the second term both in Eq. (5) and in the right hand side of Eq. (7) can be neglected, and balancing all the other terms, we obtain: $\varphi_0 \sim \mathrm{St}^{-1/3}h_0$, $l \sim \mathrm{St}^{-2/3}h_0^{3/2}$ which leads to the observed numerical scalings

$$p_0 \sim h_0^{-1/2} \text{ and } \kappa_0 \sim \mathrm{St}^{4/3}h_0^{-2}.$$

We thus deduce that this regime corresponds in fact to *thick* gas layer $h_0 \gg St^{4/3}$.

Regime II: $h_0 \gg l$: here the dominant terms balance gives: $\varphi_0 \sim \mathrm{St}^{-5/3}h_0^2$, $l \sim \mathrm{St}^{-4/3}h_0^2$ and

$$p_0 \sim \mathrm{St}^{-2/3} \text{ and } \kappa_0 \sim \mathrm{St}^{8/3}h_0^{-3}.$$

Consistently, this regime holds for *thin* gas layer $h_0 \ll \mathrm{St}^{4/3}$ and this analysis suggests that the self similar behavior observed in the numerics is valid only for large enough h_0. We predict thus another self-similar regime closer to the solid surface, not identified previously and never reached in all the numerical simulations so far.[8,10–12] In particular, it is not clear whether or not a finite time singularity would still exist (as a cusp then). Moreover, the lubrication hypothesis would not be valid anymore there, since $h_0/l \gg 1$, and full Navier-Stokes equations should be considered in the gas film.

Jet formation with surface tension: when adding the surface tension, the singularity is regularized since the high curvature regions are smoothed by the capillary pressure, as illustrated in Figure 4, where the minimal air film thickness is shown for different Weber and Stokes numbers. We observe that the dynamics separates from the $\mathrm{We} = \infty$ case when h_0 becomes small enough while the film thickness converges. As the Stokes number decreases, the dimple size decreases, and the jet appears earlier with more capillary waves. Moreover, the small angle between the tilted jet and the surface varies both with the Weber and the Stokes numbers (see Figure 5). The minimal gas layer thickness can be estimated thanks to the two different self-similar regimes exhibited for the singular case $\mathrm{We} = \infty$. Indeed, balancing the capillary term $\mathrm{We}^{-1}\kappa$ with the singular pressure gives for the gas layer depending on the regime

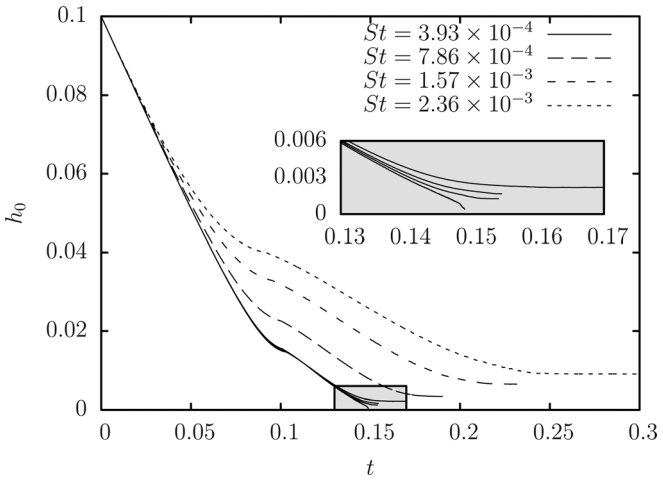

FIG. 4. Minimum gas film thickness h_0 for four different values of the Stokes number ($\mathrm{St} = 3.93 \times 10^{-4}$, 7.86×10^{-4}, 1.57×10^{-3}, 2.36×10^{-3}), as a function of time. The zoom for $\mathrm{St} = 3.93 \times 10^{-4}$ near the axis shows the evolution for different Weber number, $\mathrm{We} = 47.5$, 95, 238, and ∞ from top to bottom.

$$\mathrm{I}: \; h_0 \sim \mathrm{St}^{8/9}\mathrm{We}^{-2/3} \text{ and } \mathrm{II}: \; h_0 \sim \mathrm{St}^{10/9}\mathrm{We}^{-1/3}$$

while the two behaviors cross for $\mathrm{We} \sim \mathrm{St}^{-2/3}$ (with high Weber number for regime II). Such dependence is investigated in Figure 6, where the minimal gas thickness is compared with the predicted scalings. We find that the two exponents vary as follows $h_0 \sim \mathrm{St}^{0.9-1}\mathrm{We}^{-0.33-0.4}$ which is in reasonable agreement with regime II. Finally, taking the capillary length due to the drop deceleration $\sqrt{\gamma RH^*/\rho_l V^2} \sim \mathrm{St}^{1/3}\mathrm{We}^{-1/2}$ for the jet thickness,[15] mass conservation[16] gives for the jet velocity $V_{jet} \sim \mathrm{We}^{1/2}\mathrm{St}^{-2/3}$, in good qualitative agreement with Figure 5.

What are the main conclusions of our work? Since our two control parameters (We and St) do not vary when the gas pressure changes, compressibility of the gas was invoked before[7,8,12] as a clue to explain the splashing dependence on the gas pressure observed in the experiments.[7] However,

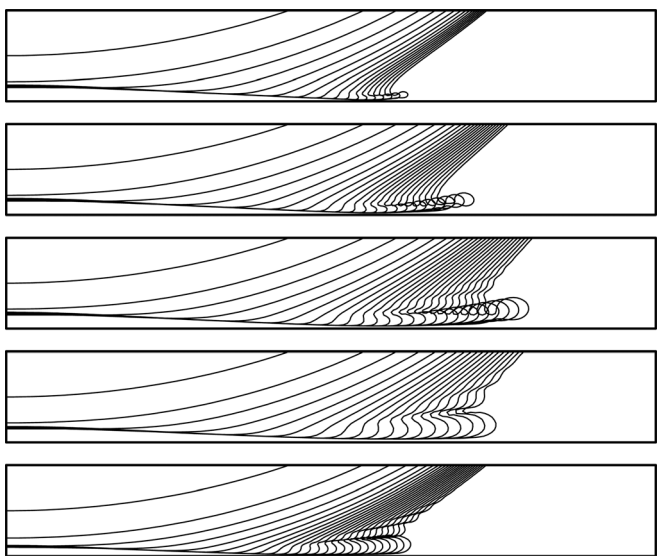

FIG. 5. Five different computations, with $\mathrm{We} = 238$, 95, 47.5, 23.7, respectively, from top to bottom and $\mathrm{St} = 1.35 \times 10^{-3}$. The bottom figure is for $\mathrm{We} = 23.7$ and $\mathrm{St} = 6.29 \times 10^{-4}$.

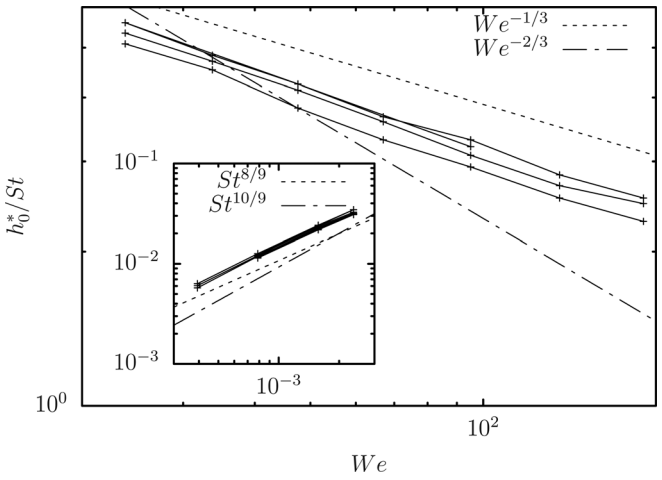

FIG. 6. Minimum gas film thickness h_0 for four different values of the Stokes number ($St = 3.93 \times 10^{-4}$, 7.86×10^{-4}, 1.57×10^{-3}, 2.36×10^{-3}), rescaled by St and not-rescaled (inset), as a function of the Weber number.

computing the minimal gas thickness in the experiments[7] following the scaling laws for h_0 obtained above, we observe that it is of the order of a few angstrom, much below the mean free path even at atmospheric pressure ($\sim$60 nm). Therefore, it is reasonable to consider that the liquid film eventually touches the solid so that the lubrication approximation made here is not valid anymore: instead we have a rapid expansion of a liquid jet in contact with the solid. Notice that such estimate would give similar conclusions if compressibility was accounted for. Although we cannot provide a final explanation for the splashing transition when the pressure varies, we want to emphasize that other physical mechanisms than compressibility should be investigated, such as the coupling between the complex dynamics of the rapidly moving contact line[17] with the surrounding gas for instance. In addition, we would like to point out that the present work exhibits the first numerical evidence of the emergence of a liquid jet within the lubrication approximation and thus the measurement of the skating height, data which could not be obtained from previous 1D numerical computations.[8,12]

Finally, since the scaling laws for h_0 are deduced before the jet formation, it is important to notice that liquid viscosity would not drastically affect the main conclusions of our calculations although it would change the jet thickness (then of order $\mathrm{St}^{1/3}\mathrm{Re}^{-1/2}$ in general much smaller than the capillary length calculated before) and the jet velocity ($\mathrm{Re}^{1/2}$).[16,18]

[1]M. Rein, "Phenomena of liquid drop impact on solid and liquid surfaces," Fluid Dyn. Res. **12**, 61 (1993).
[2]M. Coantic, "Mass transfert across the ocean-air interface: small scale hydrodynamic and aerodynamic mechanisms," PhysicoChem. Hydrodyn. **1**, 249 (1980).
[3]R. Rioboo, M. Marengo, and C. Tropea, "Outcomes from a drop impact on solid surfaces," Atomization Sprays **11**, 155 (2001).
[4]K. Range and F. Feuillebois, "Influence of surface roughness on liquid drop impact," J. Colloid Interface Sci. **203**, 16 (1998).
[5]C. Josserand, L. Lemoyne, R. Troeger, and S. Zaleski, "Droplet impact on a dry surface: triggering the splash with a small obstacle," J. Fluid Mech. **524**, 47 (2005).
[6]L. Xu, L. Barcos, and S. R. Nagel, "Splashing of liquids: Interplay of surface roughness with surrounding gas," Phys. Rev. E **76**, 066311 (2007).
[7]L. Xu, W.W. Zhang, and S.R. Nagel, "Drop splashing on a dry smooth surface," Phys. Rev. Lett. 94, 184505 (2005).
[8]S. Mandre, M. Mani, and M. P. Brenner, "Precursors to splashing of liquid droplets on a solid surface," Phys. Rev. Lett. **102**, 134502 (2009).
[9]P. D. Hicks and R. Purvis, "Air cushioning and bubble entrapment in three-dimensional droplet impacts," J. Fluid Mech. **649**, 135 (2010).
[10]F. T. Smith, L. Li, and G. X. Wu, "Air cushioning with a lubrication/inviscid balance," J. Fluid Mech. **482**, 291 (2003).
[11]A. A. Korobkin, A. S. Ellis, and F. T. Smith, "Trapping of air in impact between a body and shallow water," J. Fluid Mech. **611**, 365 (2008).
[12]M. Mani, S. Mandre, and M. P. Brenner, "Events before droplet splashing on a solid surface," J. Fluid Mech. **647**, 163 (2010).
[13]J. R. Lister, A. B. Thompson, A. Perriot, and L. Duchemin, "Shape and stability of axisymmetric levitated viscous drops," J. Fluid Mech. **617**, 167 (2008).
[14]J. Eggers, "Nonlinear dynamics and breakup of free-surface flows," Rev. Mod. Phys. **69**, 865 (1997).
[15]C. Clanet, C. Béguin, D. Richard, and D. Quéré, "Maximal deformation of an impacting drop," J. Fluid Mech. **517**, 199 (2004).
[16]C. Josserand and S. Zaleski, "Droplet splashing on a thin liquid film," Phys. Fluids **15**, 1650 (2003).
[17]K. Yokoi, "Numerical studies of droplet splashing on a dry surface: triggering a splash with the dynamic contact angle," Soft Matter **7**, 5120 (2011).
[18]A. Mongruel, V. Daru, F. Feuillebois, and S. Tabakova, "Early post-impact time dynamics of viscous drops onto a solid dry surface," Phys. Fluids **21**, 032101 (2009).